DEVELOPMENT OF A QUANTITATIVE VIDEO-BASED VISUALIZATION METHOD TO CHARACTERIZE THE FLOW BEHAVIOR OF FOOD PARTICULATES IN A MODEL CONTINUOUS ASEPTIC STERILIZER[3]

SARID M. SHEFET[1], BRIAN W. SHELDON[2], BRIAN E. FARKAS[1] and KENNETH R. SWARTZEL[1]

Departments of Food Science[1] and Poultry Science[2]
North Carolina State University
Raleigh, NC 27695-7624

Accepted for Publication April 16, 1999

ABSTRACT

The objectives of this study were to develop a quantitative visualization tool for evaluating flow behavior of particles in a compartmented aseptic system or other flow systems. The three dimensional movement of polystyrene balls as influenced by ball diameter (0.95 and 1.90 cm), fluid flow rate (10, 20 and 30 L/min) and conveyor disk design (2 configurations) was recorded in a model heating apparatus and analyzed using motion analysis software. Ball speed and net-to-gross-displacement ratio (NGDR) values were calculated for ball movement in the x;y and x;z planes. As carrier liquid flow rate increased, there was an associated increase in both the mean and standard deviation speed and NGDR values. In general, larger ball sizes yielded lower speed and NGDR values (i.e., less movement). A concave (bowl-like) conveyor disk design as opposed to a 90° flat-edge disk design yielded greater speed and NGDR values when carrier velocity was greater than 20 L/min. Speed and NGDR values having higher standard deviations were interpreted as having more compartmental mixing. Furthermore, speed and NGDR mean and standard deviations were highly correlated. The results of this study demonstrated the potential utility of the flow visualization method for quantitating the flow behavior of particles through tubes. Furthermore, this method should be of value to food process

[2] Corresponding author: Dr. Brian W. Sheldon, Department of Poultry Science, Box 7608, North Carolina State University, Raleigh, NC 27695-7608; Phone #: (919) 515-5407; FAX #: (919) 515-7070

[3] Paper number FSR98-12 of the Journal Series of the Department of Food Science, North Carolina State University, Raleigh, NC 27695-7624. The use of trade names in this publication does not imply endorsement by the North Carolina Agricultural Research Service nor criticism of similar ones not mentioned.

Journal of Food Process Engineering 22 (1999) 141–160.

engineers in developing continuous aseptic processes for particulate-containing foods.

INTRODUCTION

One of the simplest ways to commercially sterilize a food particulate or liquid containing food particulates is to apply a single thermal process to the fully blended product. Unfortunately, the use of conventional continuous pasteurization systems, which were designed primarily for liquids and semi-solids, do not currently satisfy either product quality specifications or safety requirements of U.S. regulatory agencies (Marcotte *et al.* 1994; Simunovic *et al.* 1995).

When processing particles in a dynamic system, a major challenge is to insure that the intact particles flow through the system in a homogeneous manner. For example, a major concern encountered with aseptically processed low-acid food products containing particulates is the need to sterilize the core of the particulate without over-processing the liquid or exterior of the particulate. In pasteurizing food particulates, one generally assumes that the slowest heating point (i.e., the cold spot) is at the center of the largest particle with the lowest thermal conductivity and minimum residence time (fastest moving particle). Since it is extremely difficult to assess the flow dynamics of the fluid-particulate mixture, the necessary heating that would satisfy government regulations may lead to over-processing of one ingredient while insufficiently heating others. In most cases this would result in an unacceptable product due to adverse changes in flavor, color, nutrient content and other physical or chemical properties (Burton 1988; Ramaswamy *et al.* 1995).

There are several processes designed to solve the issue of particulate processing. The best known is the Jupiter system which is based on the principle of sterilizing the component solids and liquid separately and then mixing them together in a sterile environment before filling into containers (Holdsworth and Richardson 1989). The system was not commercially profitable since the solids had to be sterilized in batches. Systems that employ unconventional means of heating such as the Ohmic heating system (APV) which utilizes electrical resistance heating and the Multitherm system (Alfa Star) which incorporates microwave heating (Biss *et al.* 1989) were not commercially successful since nonionic materials such as fats, oils, sugars, syrups or tap water without added salts are not suitable conductors in either system. The above two systems as well as some other attempts to modify swept or scraped surface heat exchangers and tubular heat exchangers to handle particles were not able to comply with the Food and Drug Administration's (FDA) requirements for proving residence time distribution (Hirahara 1980; Hersom 1985; Sawada and Merson 1986; Hermans

1991; Dennis 1992). A recent workshop conducted jointly by the National Center for Food Safety and Technology (NCFST) and the Center for Aseptic Processing and Packaging Studies (CAPPS) developed a case study which served as a framework for a validation study for filing with the FDA. Based on the case study, a scheduled process for the aseptic processing and packaging of potato soup was developed by Tetra Pak Inc. and filed with the FDA. They received a "no rejection" letter from the agency on May 31, 1997 (Palaniappan and Sizer 1997; Rice 1997). As important as this development may appear, the protocol was only approved for a specific product with a specified particle size. The application of this protocol to other products and other sized particles will not necessarily gain FDA approval since a change in any of the above parameters will effect the residence time of the particles.

A potential solution to the above problem was suggested in a recently issued patent under the title of 'Hydrostatic Heating Apparatus' (Shefet 1996). The apparatus comprises an enclosed chamber which is open to atmospheric pressure and contains a hydrostatic liquid (i.e., heating media such as water, sauce, or gravy). The enclosed chamber has a product inlet [i.e., formulated two-phase suspension such as meat and gravy or particulates (i.e., potato) suspended in a heating/carrier liquid such as water] and outlet openings and also a heating zone positioned between the two product openings. The apparatus is also equipped with a transporting device such as a conveyor positioned in the enclosed chamber which extends through the heating zone and serves to convey the particulate product in the liquid through the apparatus. The apparatus maintains the particulate product in the liquid under hydrostatic pressure while in the heating zone. The apparatus may be used in combination with an aseptic packager connected to the enclosed product outlet opening for aseptically packaging the particulate product.

Flow visualization has contributed greatly to the development of modern fluid dynamics and has been utilized by such pioneers as O. Reynolds, L. Prandtl and others. Flow visualization is capable of revealing the entire flow profile and plays an important role in understanding flow phenomena. Complex flow phenomena such as the transition from laminar to turbulent flow in a tube, which cause sudden pressure drops and the formation of Karman vortices can be understood from flow visualization photographs obtained by various techniques (Chung 1989).

For complex fluid flows it is difficult to understand the entire flow profile by using just probes for measuring flow velocity, direction, and other quantitative values. Thus, other tools such as flow visualization methods to characterize the entire flow pattern represent a powerful tool to complement the probe method. Generally, fluid motion is invisible and thus can not be visualized without first making the flow visible such as by introducing tracers (Taneda 1985).

An array of video/photographic-based visualization methods are available using tracers introduced in water or in other liquids. It should be noted that visualization methods used to monitor elements suspended in fluid are in some cases limited by the variations between the trajectories of the particles and of the fluid elements they represent. This problem is mainly associated with particles not having the same density and viscosity as the fluid. Because particles often have different diameters, they are subjected to averaging effects. They are also affected by centrifugal or centripetal forces and gravity effects. It should be noted that the trajectories and emission lines of effective tracers coincide with the streamline of a steady flow, at least in the laminar flow regime. This is not true for an unsteady flow or in the case of a turbulent flow regime. Provided that some precautions are taken, tracers may give an accurate picture of the instantaneous or averaged flow (Werlé 1974).

Some commonly used solid tracers which are generally introduced by a probe upstream of the model include glass balls, perspex powder, aluminum particles and spherical polystyrene beads of a density similar to that of water (Werlé 1989). Aluminum and magnesium flakes, 20 to 50 μm long and about 5μm thick, are nonspherical tracers which have been used on many occasions for studying hydrodynamics. With appropriate illumination these particles generate excellent flow pictures as documented in many studies (Merzkirch 1987). Salengke and Sastry (1995) used vidęo visualization in their studies to determine the effect of particle size and flow rate on residence time distribution (RTD). Their visualization method was similar to the one used by Lee *et al.* (1995) in which an acrylic outer shield applied to a scraped surface heat exchanger was used to view the effect of particles on the liquid RTD.

The focus of this research was to develop a video-based quantitative tool for evaluating flow behavior of particles in the model hydrostatic heating apparatus or in any other heating tube. This tool may be useful for characterizing and comparing flow behavior of particles in different aseptic processing systems containing liquid and particles. Furthermore, this method will allow process engineers to make recommendations on specifications (i.e., conveyor disk design, liquid velocity, particulate load, etc.) of future designs of the hydrostatic heating apparatus or any other system designed for conveying particulates.

THEORY

A continuous method based on the hydrostatic heating apparatus design for commercially sterilizing fluids containing particles was hypothesized by the authors. The method assumes that a 12 *D* (decimal reduction) reduction in a target bacterial spore population is attained by exposure to 121C for 3 min (or an equivalent time/temperature process) (Ramaswamy *et al.* 1995) and that the standard cooking procedure of the targeted food product requires the immersion

of the product in boiling water for 7-10 min (i.e., pasta products, cooked vegetables). A thermal process yielding a F_0 value [the equivalent time in minutes at a reference temperature (i.e., 121C) to reduce the number of spores/vegetative cells of a given organism as defined by a given z value] of 3 is required from a food safety stand point for reducing *Clostridium botulinum* spore populations, although a F_0 of 5 is recommended for inactivating bacterial spores responsible for food spoilage (Lund 1975).

Under standard atmospheric pressure conditions (1 atmosphere of pressure) water boils at 100C. Boiling can also be achieved at 126C under 2.38 atm (35 Psi) or at other pressure/temperature combinations. The proposed continuous sterilization process is designed to operate at atmospheric pressure and achieves the required higher processing pressures using a liquid column of a defined height. For example, a column of water at either 10.33 or 14.24 m high has 2.0 or 2.38 atmospheres of pressure, respectively, at the base of the column (Smith and Van Ness 1987).

Considering the above, a 'U'-shaped sterilization apparatus was hypothesized as a functional design for sterilizing particulates in a fluid medium. The theoretical apparatus would be composed of two 15.5 m vertical columns containing water to a height of 14.24 m. The columns would be connected at the bottom with a horizontal pipe. The pressure at any point across the horizontal tube would equal 2.38 atm. At this elevated pressure, the boiling point of water is 126.28C.

A conveying system designed to produce individual compartments would be included in the system to carry food particles through the apparatus and into the aseptic packaging zone. Water will serve both as a sterilizing medium and as a barrier between the open environment and the aseptic zone. The design configuration and speed of the conveyor and product inlet pump would control the dwell time of the particulates in the heating zone, a fact that would assure their commercial sterility at the end of the process. The horizontal tube will act as a holding section; thus the tube length, the speed of the conveyor and the water temperature will need to be considered in assessing the lethality of the process. Based on the above process, a U.S. patent titled 'Hydrostatic Heating Apparatus' was granted (Shefet 1996).

In order to simplify the evaluation and characterization of the described device, a pilot plant model composed of a stationary conveyor system was designed and constructed (Fig. 1). In a commercial system that would contain a moving conveyor, the inlet liquid flow rate would be maintained at a constant velocity (V_i) while the cable-conveyor velocity (V_c) would always be maintained at a higher speed ($V_c > V_i$). In the stationary conveyor test model, liquid was pumped at a speed equal to the difference between V_c and V_i. This rate would be equivalent to the relative velocity of the fluid in a commercial system configured with a moving conveyor.

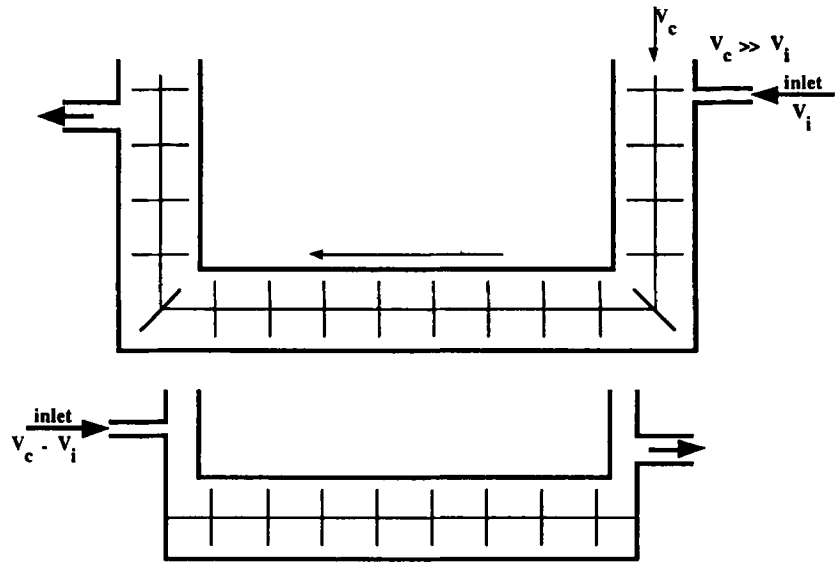

FIG. 1. A COMPARISON OF A HYDROSTATIC HEATING APPARATUS SYSTEM WITH A MOVING CABLE-CONVEYOR (TOP) AND A MODEL SYSTEM WITH STATIONARY DISKS (BOTTOM)
(v_c: Cable Conveyor Velocity, v_i: Inlet Liquid Flow Rate).

MATERIALS AND METHODS

Pilot Plant Model

A model hydrostatic heating apparatus was constructed from a 162.5 cm long, 12.7 cm I.D. clear plexi-glass tube having a wall thickness of 0.64 cm. A 90° PVC elbow (12.7 cm I.D.) was attached to each end of the tube with the inlet and outlet ends oriented downward and upward, respectively (Fig. 2). The inlet was connected to a positive-displacement pump using a 275 cm long (6.35 cm I.D.) flexible tygon tubing whereas the outlet end was positioned immediately above a 100 L stainless steel collection vat. The vat was attached to the pump inlet via a 100 cm long (6.35 cm I.D.) stainless steel pipe. The vat served to collect the water overflow from the tube during test runs. A 198 cm long (1.27 cm diameter) stainless steel rod containing five fixed PVC disks spaced 25.4 cm apart was positioned in the center of the horizontal tube using two 3.0 cm long PVC tubes (1.5 cm I.D.) glued to the inside wall of each elbow. Three disk

designs were machined and tested in this study. Their dimensions are described in the following section.

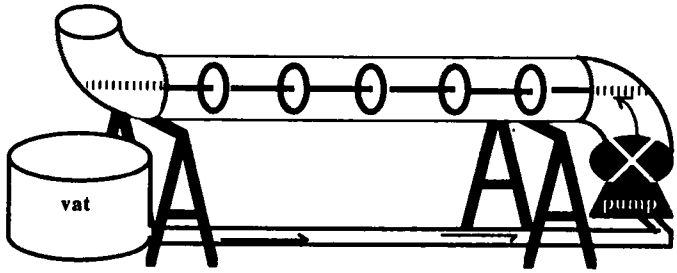

FIG. 2. GENERAL DESIGN OF THE MODEL PILOT PLANT HYDROSTATIC HEATING APPARATUS

All disks were machined from PVC sheet stock. Disk A (Fig. 3) had the simplest design consisting of flat edges and faces. Each disk was machined to be 11.43 cm in diameter, 1.27 cm thick and contained a 1.27 cm diameter hole bored through the geometric center of the disk. To add support and facilitate attachment to the stainless steel rod, a 1.27 cm PVC collar measuring 3.81 cm in diameter and having a 1.27 cm center hole was machined and centrally mounted to the back of the each disk using an adhesive. The disks were fixed to the support rod by a stainless steel set screw that was threaded through the collar perpendicular to the rod.

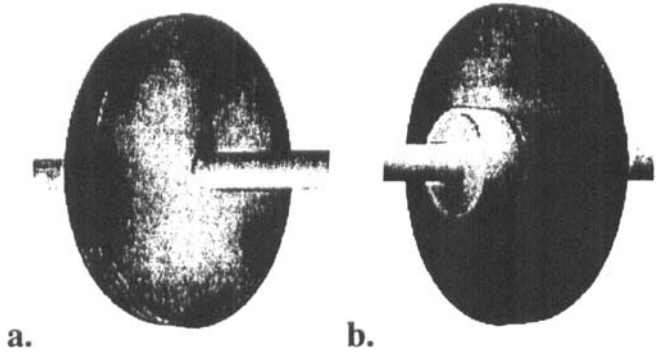

FIG. 3. VIEW OF 'DESIGN A' DISK MOUNTED ON A STAINLESS STEEL ROD (a. front view, b. Back view).

Disk B was designed in a bowl-like shape to create more mixing and turbulence in the liquid/particulate flow (Fig. 4). The disks were machined similarly to disk A with the following exceptions. Disk thickness was increased to 1.90 cm to add strength and to facilitate creating the bowl-like contour. The disk edge was cut at a 15° angle from the leading to trailing disk faces. The curvature was created using 1.90 cm and 2.22 cm ball endmills. The 1.90 cm endmill was used to curve the initial surface between the groves at 2.53 and 4.75 cm from the disk center. The remaining uncut surface between the grooves was bored out using the 2.22 cm ball endmill.

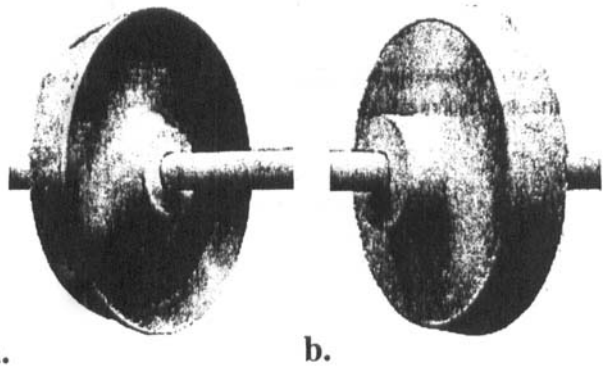

FIG. 4. VIEW OF 'DESIGN B' DISK MOUNTED ON A STAINLESS STEEL ROD
(a. Front View, b. Back view).

Similar to disk B, disk C was designed to increase mixing and turbulence of the liquid and particulates. These disks were machined to a thickness of 1.27 cm and contained 16 - 45° diagonally cut grooves, spaced 22.5° apart from each other on the leading edge of each disk (Fig. 5). The grooves were cut using a 1.90 cm endmill positioned at a 45° angle to the leading disk surface.

Pump

The positive displacement pump system used in these studies consisted of a RELIANCE® 1,730 RPM, frame model 184TC, type P-F motor (Reliance Electric Company, Columbus IN), a GNH® model GHP 2025A rotary pump (GNH Product Group, Kenosha, WI), and a Reeves® motodrive® gear drive (Reliance Electric Company, Columbus, IN) which was operated in a fully opened position. The motor speed was controlled by a variable frequency controller (model SP500 EASY CLEAN PLUS™ VS DRIVE, 146 - 1751 RPM) (Reliance Electronics, Athens, GA). In all test runs flow rate was verified using a time/volume measurement technique.

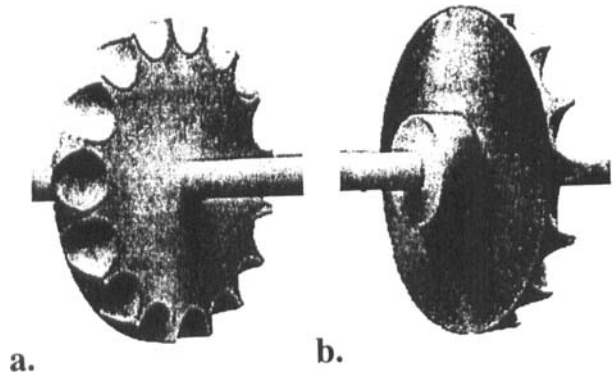

FIG. 5. VIEW OF 'DESIGN C' DISK MOUNTED ON A STAINLESS STEEL ROD (a. front view, b. back view).

Visualization

To monitor and record particulate movement, a video camera (model 1CVC2030E color video camera, General Electric Company, Portsmouth, VA) was mounted 175 cm in front of the flow test model with the lens aligned on the same horizontal plane as the tube. The camera was attached to a video recorder (VP5410TE HI speed video search VHS, Quasar, Japan). In order to view the 3-dimensional flow of a specific section of the plexi-glass tube, a mirror was aligned at a 45° angle and positioned beneath the tube. In this camera to tube and mirror orientation, the *x;y* plane was observed directly while the *x;z* plane was viewed through the reflection in the mirror (Fig. 6). A 1000W halogen light bulb positioned behind the GE Color video camera was used to illuminate the apparatus.

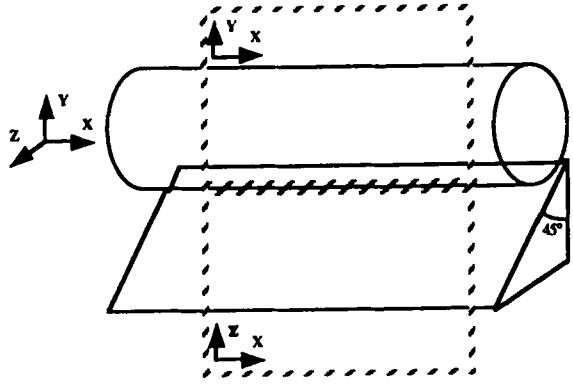

FIG. 6. GENERAL PLACEMENT OF A MIRROR BENEATH THE PLEXI-GLASS TUBE TO SIMULTANEOUSLY VIEW THE *x;y* AND *x;z* PLANES

Analysis

Each tape was replayed through a video processor (VP110, Motion Analysis Corporation, Santa Rosa, CA) which determines the pixel coordinates at which transitions occur between light and dark regions. This information is transmitted to PC-based ExpertVision™ software (ExpertVision™, Motion Analysis Corporation) where the two-dimensional coordinates of each observed object are determined by calculating the centroid of each ball outline for each digitized video frame. The output from the software included the coordinates for the $x;y$ and $x;z$ planes, particle speed and net-to-gross-displacement ratio (NGDR) of the particle. The software computes the speeds of the particles in distance per unit time (e.g. second) along a path. Speed is always positive or zero. In addition, the NGDR is computed for specific particles moving on a given path. For a given point in a path, the net displacement is the distance along a straight line from the first point of the path to the given point. In contrast, the gross displacement is the distance traveled along the actual path from the first point to the given point. The ratio between these two quantities is termed the net-to-gross-displacement ratio (Motion Analysis Corporation, 1990).

Qualitative and Quantitative Visualization Protocol

In preliminary studies designed to view flow patterns and develop general operating conditions, 70 g of Unique™ foil confetti (Unique Industries Inc., Philadelphia, PA) were introduced into the flow test apparatus by dispersing it in the overflow vat (Fig. 2). The pump was operated at several different speeds producing predetermined flow velocities. For each test run the flow apparatus was loaded with 5 disks of the same design and water pumped at a velocity of 10-40 L/min for a 5 min test period. Disk C was mounted on the stainless steel rod in two different orientations, forward and backward. The camera was positioned in front of the middle disk chamber and recorded the flow characteristics of the foil confetti.

For the quantitative trials, 0.95 cm or 1.90 cm diameter machine finish polystyrene balls having a specific gravity of 1.0 (Machining Technologies, Elmore, OH) were used. For each test run, five balls (1 black, 4 white) of the same size were introduced into each disk chamber as the rod and disks were positioned in the flow apparatus. For each ball size, four test trials of 15 min durations were conducted at three different flow rates (10, 20 and 30 L/min). Three 30 s long video segments were randomly chosen, digitized and analyzed with the motion analysis software at a frame rate of 1/30 of a second. The software output included ball speed, NGDR and exact location coordinates of the marked ball in every frame ($x;y$ and $x;z$ planes). The mean and standard deviations of the above parameters were calculated and statistically compared.

General Experimental Design and Statistics

The data were arranged in a 12 factorial design based on two ball sizes (0.95 and 1.90 cm diameter), two disk designs (A and B) and three flow rates (10, 20 and 30 L/min). Each combination was composed of 3 sets of data based on 900 consecutive observations per data set. Means, standard deviations and minimum and maximum values for both ball speed and NGDR were calculated for each data set. No significant differences were detected between the three data sets ($p \leq 0.05$) and thus they were pooled, averaged, and their means compared. Differences in mean and standard deviations for particle speed and NGDR values were determined by comparing each mean pair using the Student's t-test at $p \leq 0.05$ (LSD). Correlations between mean and standard deviation values and $x;y$ and $x;z$ plane data were calculated based on a simple linear correlation coefficient procedure (SAS Institute 1993; Steel and Torrie 1980).

RESULTS AND DISCUSSION

Qualitative Visualization

The effects of four disk designs and four water velocities (10, 20, 30 and 40 L/m) on confetti flow patterns were investigated in the test apparatus by monitoring the video recordings of 16 test runs (Fig. 7). A typical flow profile of the four disk designs consisted of an acceleration of the confetti velocity as it approached and passed through the gap between the disk and the tube wall. On the trailing side of the disk the confetti velocity decreased with some following a path parallel to the inner tube wall while another portion was pulled

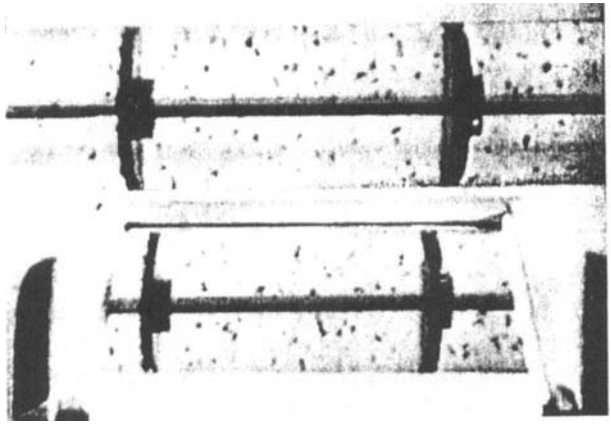

FIG. 7. A GENERAL FRONT VIEW OF THE TUBE (TOP VIEW) AND THE REFLECTING MIRROR (BOTTOM VIEW) AS OBSERVED IN THE QUALITATIVE VISUALIZATION STUDIES

into a whirlpool-like motion immediately behind the disk. Regardless of the disk design, an increase in fluid velocity resulted in higher turbulence in the compartments. Confetti flow patterns did not vary appreciably across the four disk types. Disk A (90° edges) resulted in a circular confetti flow pattern downstream of each disk which continued over a third of the downstream compartment. With disk B (bowl shape), the circular flow pattern continued over approximately two-thirds of the downstream compartment. Disk C (diagonally-cut grooves) resulted in a similar flow pattern as disk A except that it extended over half of the downstream compartment. When disk C was mounted in a reverse configuration (grooves on the trailing disk face), no significant changes in the flow pattern were observed except for the appearance of a strong current along the trailing edge of the disk.

The area between the inner tube wall and the center rod is 125.41 cm^2 per compartment and approximately 24.07 cm^2 between the tube wall and the disk edge. Since mass flow in the apparatus is known, the speed (v) of the liquid can be calculated using the mass flow (1) and mass balance (2, 3) equations.

$$\dot{m} = A \times v \times \rho \tag{1}$$

$$A_1 \times v_1 \times \rho_1 = A_2 \times v_2 \times \rho_2 \tag{2}$$

or

$$A_1 \times v_1 = A_2 \times v_2 \tag{3}$$

Using the above equations, the water flow velocity through the disk gap was estimated to be approximately 5.2 times faster than the average velocity up or downstream of the disk. This calculation agrees with the observed increase in confetti velocity as it passed through the disk gap. This qualitative assessment indicates that disk design, as opposed to increasing flow rate, had a greater influence on creating more compartmental mixing. Disk B appears to have created the greatest mixing conditions. Based on these preliminary studies it was decided to limit the quantitative experiments to examining only disk A and B at flow rates of 10, 20 and 30 L/min.

Quantitative Visualization

The ball coordinates from all test runs were plotted as illustrated in Fig. 8. Balls exposed to lower flow rates (Fig. 8a) had more concentrated plot profiles or less overall movement than balls exposed to higher flow rates (Fig. 8b).

Since an objective of the present study was to identify and recommend process parameters (i.e., disk configuration, flow rate) leading to maximum

particle distribution and mixing in the hydrostatic heating apparatus, a large standard deviation of the test parameters was desirable and indicated greater particle mixing. For particle speed, large standard deviations indicate a wide range in particle velocities. As for NGDR, a larger standard deviation is associated with more changes in ball position over time.

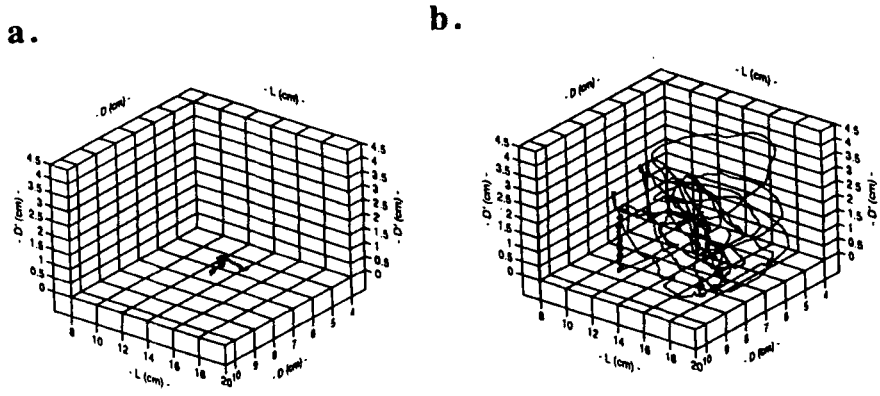

FIG. 8. EFFECT OF FLOW RATE ON BALL MIGRATION PATTERNS OBTAINED FROM *XY* AND *XZ* COORDINATES (30 s sample; n=900; 0.95 cm DIAMETER BALL; DISK DESIGN B)
a. 10 L/min Flow rate. b. 30 L/min flow rate

Speed

A high degree of correlation was detected between the *x;y* and *x;z* speed means and standard deviations. A comparison between the *x;y* and *x;z* planes, sorted by ball size and disk design, yielded r^2 values ranging from 0.902 to 0.999 for the mean speeds and 0.835 to 0.996 for the standard deviation values. Within the *x;y* plane, the mean speed was highly correlated to the standard deviations with r^2 values ranging from 0.975 to 0.999, while those in the *x;y* plane yielded values ranging from 0.954 to 0.998. These high correlations between *x;y* and *x;z* planes suggest that only one plane needs to be monitored in this system. Furthermore, higher mean ball velocities also yielded a larger variation in ball velocities.

In general, the concave shape of disk B yielded higher mean ball speeds than disk A. Furthermore, smaller diameter balls and increased flow velocities, especially at 30 L/min, resulted in faster ball speeds and greater variation in ball speeds (Fig. 9).

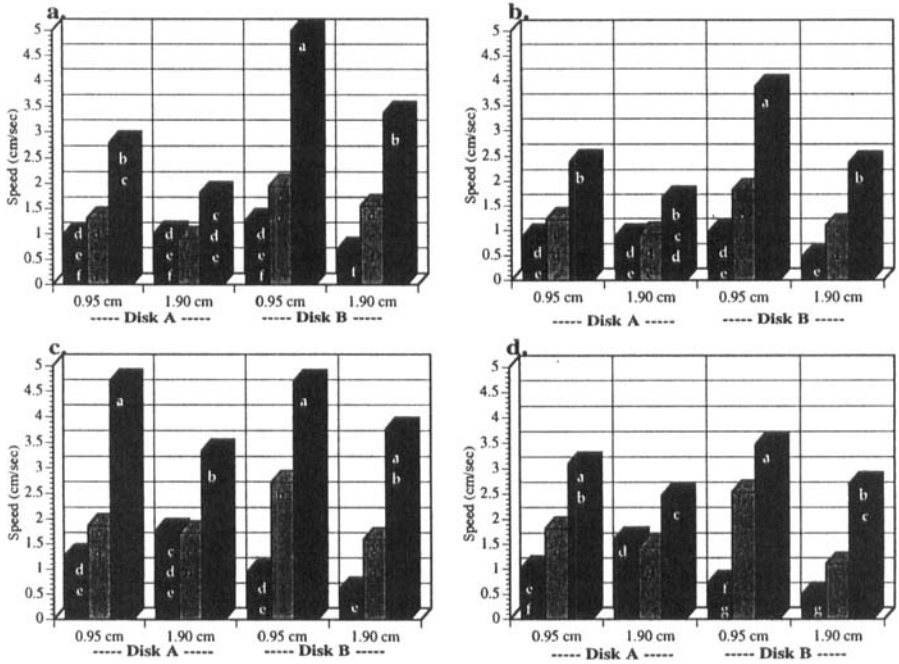

FIG. 9. EFFECT OF DISK DESIGN AND LIQUID FLOW RATE ON THE MEAN SPEED AND STANDARD DEVIATION OF DIFFERENT DIAMETER POLYSTYRENE BALLS IN THE *x;y* AND *x;z* PLANES

Means (n=2,700) with different letters are significantly different. a. Mean *x;y*, b. Standard deviation *x;y*, c. Mean *x;z*, d. Standard deviation *x;z*;
$P \leq 0.05$, ■10 L/min, ■ 20 L/min, ■ 30 L/min.

For disk B, the average speed and standard deviation of the 0.95 cm diameter ball in the *x;y* plane were significantly higher at 30 L/min than any other ball size / disk design / liquid flow rate combination (4.99, 3.88 cm/s, respectively) (Fig. 9a,b). Within disk B, for both 0.95 and the 1.90 cm diameter balls, the 30 L/min flow rate also yielded significantly higher ball speeds (4.99, 3.36 cm/s, respectively) and standard deviations (3.88, 2.36 cm/s, respectively). No significance different in mean ball speeds were detected between the 10 and 20 L/min flows for disk B. Although both ball sizes had similar specific gravities (~ 1.0), the speed of the smaller spheres at 30 L/min was significantly faster than the 1.90 cm balls. This data agrees with the qualitative data generated using the foil confetti in which faster flow yielded faster confetti movement.

With some exceptions, the mean ball speeds recorded in the *x;z* plane followed the same patterns as the ball speeds observed in the *x;y* plane (Fig. 9a,c). This observation is supported by the high correlation ($r^2 > 0.9$) detected between the *x;y* and *x;z* speed data. The mean and standard deviation ball velocities at 30 L/min for disk A were higher ($P > 0.05$) in the *x;z* plane (4.70, 3.09 cm/s, respectively for the 0.95 cm ball and 3.33, 2.46 cm/s respectively, for the 1.90 cm ball) than observed in the corresponding *x;y* plane (2.73, 2.38 cm/s, respectively for the 0.95 cm ball and 1.81, 1.66 cm/s respectively, for the 1.90 cm ball) (Fig. 9). Within ball size and flow rate, disk type generally did not significantly influence the mean ball speed and standard deviations. Within disk A and the *x;z* plane, the average speed of the 0.95 cm balls at a flow velocity of 30 L/min was significantly faster (4.7 cm/s) than the speed of the 1.90 cm balls (3.33 cm/s) (Fig. 9c). The corresponding standard deviations followed the same trends as observed for the mean speeds. The 0.95 cm ball standard deviations (3.09 cm/s) were significantly higher than the 1.90 cm balls (2.46 cm/s) at 30 L/min (Fig. 9d). It appears that a combination of disk B and exposure to flow velocities equal to 30 L/min exert a greater influence on the *x;y* plane ball speed than detected with disk A. This may be a direct result of the concave shape of disk B.

NGDR

Similar to ball speed, an increase in flow velocity from 10 to 30 L/min resulted in an increase in the mean *x;y* plane NGDR value for the 0.95 cm balls (disk A) and 1.90 cm balls (disk B), and 0.95 (disk A) and 1.90 cm balls (disk A and B) in the *x;z* plane (Fig. 10). The larger the NGDR value, the greater the movement of the polystyrene balls. Mean and standard deviation NGDR values within and across planes were highly correlated ($r^2 > 0.93$) for the 0.95 cm balls (disk A) and 1.90 cm balls (disk B).

Increasing flow velocities had its greatest impact on NGDR values across planes with the 1.90 cm ball and disk B combination (Fig. 10a). With this combination, NGDR values increased significantly over the three flow velocities. The overall mean distance the ball traveled (i.e., NGDR value) was not generally influenced by disk configuration or ball size. Some exceptions included the following test configurations: 1.90 cm balls, 30 L/min, disk A vs disk B (*x;y* plane); and 10 and 20 L/min, disk B, 0.95 vs 1.90 cm balls (*x;y* plane). In the first exception, disk B resulted in greater ball movement than disk A. For the other two exceptions, the smaller ball traveled significantly greater distances. NGDR standard deviation values were not influenced by flow velocity, ball size or disk shape (Fig. 10b).

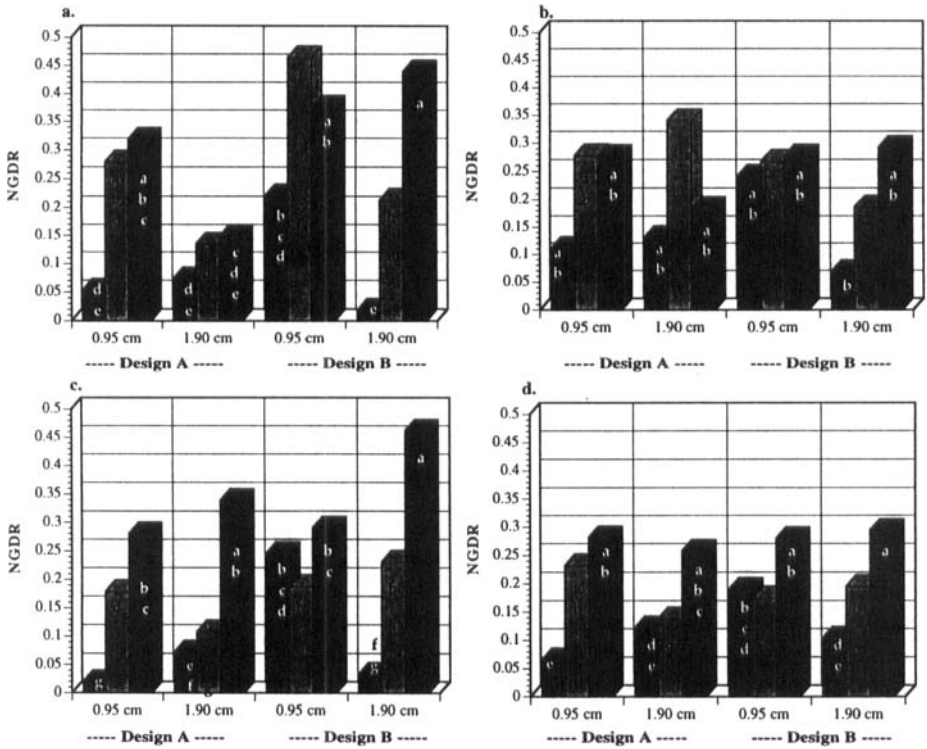

FIG. 10. EFFECT OF DISK DESIGN AND LIQUID FLOW RATE ON THE MEAN NET-TO-GROSS-DISPLACEMENT-RATIO (NGDR) AND STANDARD DEVIATION OF DIFFERENT DIAMETER POLYSTYRENE BALLS IN THE *x;y* AND *x;z* PLANES
Means (n=2,700) with different letters are significantly different. a. Mean *x;y*, b. Standard deviation *x;y*, c. Mean *x;z*, d. Standard deviation *x;z*;
$P \leq 0.05$, ■10 L/min, ■ 20 L/min, ■ 30 L/min.

In the *x;z* plane, flow velocity significantly influenced the mean NGDR values for the 0.95 and 1.90 cm balls and disk A combinations and 1.90 cm balls and disk B combination (Fig. 10c). The higher the flow velocity, the greater the ball movement. Furthermore, smaller balls moved greater distances in both planes than larger balls for the 10 L/min and disk B combination. The reverse was true at 30 L/min (*x;z* plane). Disk B also generated more overall movement of the 0.95 cm balls in the *x;z* plane at 10 L/min than disk A. NGDR standard deviations were not influenced by flow rate, ball size or disk shape (Fig. 10d).

In summary, disk design influenced both ball speed and NGDR means at the 30 L/min flow rate. The concave shape of disk B produced more flow variations than the flat face configuration of disk A. Thus, the B disk design would be recommended for situations in which greater mixing is required within compartments. Another anticipated conclusion is that in most cases increases in flow velocity resulted in significantly higher speed and NGDR means and standard deviations. This finding suggests that an increase in cable conveyor speed will result in greater mixing within the compartments of the hydrostatic heating apparatus or other compartmented flow configurations. Graphs of the speed and NGDR mean and standard deviations for both the 0.95 and 1.90 cm diameter balls produced similar patterns under the same operating conditions. While having similar densities, it appears the smaller balls at the highest flow velocity were subjected to more movement and agitation than the larger balls. This may be explained by the fact that smaller shapes are less likely to be captured between two different streams/forces at the same time (Werlé 1989). The high correlation detected between the *x;y* and *x;z* plane values (mean and standard deviation speed and NGDR values) indicated that future flow recordings may only require measurement in one plane. Based on these findings, the quantitative flow visualization method described in this study appears to be an excellent analytical tool for describing the three dimensional movement and behavior of particles in a fluid stream. Previous visualization of fluid systems investigations have demonstrated that particle flow behavior can be visualized qualitatively (Lee *et al.* 1995; Salengke and Sastry 1995). The visualization and analysis methods used in this present study yielded both qualitative and quantitative data.

In future applications, the flow visualization and measurement methods employed in this study may be useful for comparing and contrasting the flow characteristics of different pasteurization systems or any other system involving liquid flow. The basis of these comparisons would be the calculated mean speed and NGDR values and their standard deviations. Since these methods offer an objective numerical comparison as opposed to the standard subjective visualization procedures, the investigator is provided with more objective information that can be used in system design as well as aiding regulatory approvals. For example, speed and NGDR values having small standard deviations may describe systems having more uniform flow characteristics and less mixing.

Based on the successful assessment of the quantitative flow visualization tool in this study, it is anticipated that this method may be useful for comparing flow characteristics of particles in other food conveying systems (i.e., continuous aseptic pasteurizers). The fact that the movement of a particle in a given system can be documented and characterized suggests that similar comparisons of particle movements can be achieved in other systems or factors influencing flow can be readily evaluated. Furthermore, this method will allow process engineers

to make recommendations on specifications (i.e., conveyor disk design, liquid velocity, particulate load, etc.) of future designs of the hydrostatic heating apparatus or any other system designed for conveying particulates.

ACKNOWLEDGMENTS

We thank Dr. Dan Kamykowski, Head of the Phytoplankton Research Lab, Department of Marine, Earth and Atmospheric Sciences, North Carolina State University, for his suggestions and the use of the Motion Analysis equipment. In addition, we thank Dr. Larry F. Stikeleather, Department of Biological and Agricultural Engineering, North Carolina State University, for his insightful recommendations. The authors also wish to thank Ms. Susan Hale for her excellent technical assistance.

NOMENCLATURE

A Area, m^2
$\dot{m}$ Mass flow rate, kg/s
v Velocity, m/s
ρ Density of the liquid medium, kg/m^3
v_c Cable conveyor velocity, m/s
v_i Inlet liquid flow rate, kg/s

REFERENCES

BISS, C.H., COOMBES, S.A. and SKUDDER, P.J. 1989. The development and application of Ohmic heating for the continuous heating of particulate foodstuffs. In *Process Engineering in the Food Industry - Development and Opportunities*. (R.W. Filed and J.A. Howell, eds.) pp. 17-26, Elsevier Applied Science, London.

BURTON, H. 1988. *Ultra High Temperature Processing of Milk and Milk Products*. Elsevier Applied Science, Barking, U.K.

CHUNG, K.C. 1989. Internal flow. In *Handbook of Flow Visualization*, (W. J. Yang, ed.) pp. 415-457, Hemisphere Publishing Corp., New York.

DENNIS, C. 1992. HTST processing - scientific situation and perspective of the industry. In *Processing and Quality of Foods* part 1, (Zeuthen *et al.* eds.) Elsevier Applied Science, London.

FOGIEL, M. 1993. *The Transport Phenomena Problem Solver*. Research and Education Association, Piscataway, NJ.

HERMANS, W.F. 1991. Single-flow fraction specific thermal processing (Single-Flow FSTP) of liquid foods containing particulates. News in aseptic processing and packaging. In *Proceedings of Technical Research Center of Finland*. pp. 35–43, VTT Symposium 119. Espoo, Finland.

HERSOM, A.C. 1985. Aseptic processing and packaging of food. Food Rev. Intl. *1*(2), 215–270.

HIRAHARA, K. 1980. Continuous pressure cooking apparatus. US Patent 4,181,072.

HOLDSWORTH, S.D. and RICHARDSON, P.S. 1989. Continuous sterilization operations for aseptic packaging: an overview. In *Process Engineering in the Food Industry - Development and Opportunities*. (R. W. Filed and J. A. Howell, eds.) pp. 3–16, Elsevier Applied Science, London.

LEE, J.H., SINGH, R.K. and LINEBACK, D.S. 1995. Particle concentration influence on liquid residence time distribution in a model aseptic processing system. J. Food Process Engineering *18*, 119–133.

LUND, D.B. 1975. Heat processing. In *Principles of Food Science* Part II. (O. K. Fennema, ed.) pp. 31–92, Marcel Dekker, New York.

MARCOTTE, M., RAMASWAMY, H.S. and ABDELRAHIM, K.A. 1994. Aseptic processing of particulate foods. Alimentech Food research and development centers industry liaison newsletter. Agriculture and Agri-Food Canada Research Branch. *2*(7), 12–13.

MERZKIRCH, W. 1987. Addition of foreign materials. In *Flow Visualization*. (W. Merzkirch, ed.) pp. 2–53, Academic Press, Orlando, FL.

Motion Analysis Corporation. 1990. ExpertVision™ Reference Manual. Motion Analysis Corporation, Santa Rosa, CA.

PALANIAPPAN, S. and SIZER, C. E. 1997. Aseptic process validated for foods containing particulates. Food Tech. *51*(8), 60–68.

RAMASWAMY, H.S., ABDELRAHIM, K.A., SIMPSON, B.K. and SMITH, J.P. 1995. Residence time distribution (RTD) in aseptic processing of particulate foods: a review. Food Res. Intl. *28*(3), 291–310.

RICE, J. 1997. Chunky potato soup garners aseptic approval. Prepared Food. *166*(11), 93.

SALENGKE, S. and SASTRY, S.K. 1995. Residence time distribution of cylindrical particles in a curved section of a holding tube: The effect of particle size and flow rate. J. Food Process Engineering *18*, 363–381.

SAS INSTITUTE INC. 1993. JMP® User's guide Ver. 3. SAS Institute Inc., Cary, NC.

SAWADA, H. and MERSON, R.L. 1986. Estimation of process conditions for bulk sterilization of particulate foods in water-fluidized bed. In *Food Engineering and Process Applications*. Vol. 1. Transport Phenomena. pp. 569–581, Elsevier Applied Science, London.

SHEFET, S. M. 1996. Hydrostatic heating apparatus. US patent 5,546,849.

SIMUNOVIC, J., ABDEL-RAHIM, K., KYEREME, M. and SMITH, E. 1995. Private communication. Department of Food Science, North Carolina State University, Raleigh, NC.

SMITH, J.M. and VAN NESS, H.C. 1987. Steam tables. In *Introduction to Chemical Engineering Thermodynamic*. (J.M. Smith and H.C. Van Ness, eds.) pp. 573–675, McGraw-Hill Pub., New York.

STEEL, R.G.D. and TORRIE, J.H. 1980. *Principles and Procedures of Statistics Abiometric Approach*, 2nd Ed., McGraw-Hill Pub., New York.

TANEDA, S. 1985. Flow field visualization. In *Theoretical and Applied Mechanics*. (F. I. Niordson and N. Olhoff, eds.) pp. 399–410, Elsevier, New York.

WERLÉ, H. 1974. Le tunnel hydrodynamique au service de la recherche aérospatiale, ONERA Publ. 156.

WERLÉ, H. 1989. Liquids. In *Handbook of Flow Visualization*. (W. J. Yang, ed.) pp. 41–44, Hemisphere Pub., New York.